

Novel Topology and Control Strategy of HVDC Grid Connection for Open Winding PMSG based Wind Power Generation System

Hengli Zeng * and Heng Nian **

Abstract – To satisfy the high voltage direct current (HVDC) grid connection demand for wind power generation system, a novel topology and control strategy of HVDC grid connection for open-winding permanent magnet synchronous generator (PMSG) based wind power generation system is proposed, in which two generator-side converter and two isolated DC/DC converters are used to transmit the wind energy captured by open winding PMSG to HVDC grid. By deducing the mathematic model of open winding PMSG, the vector control technique, position sensorless operation, and space vector modulation strategy is applied to implement the stable generation operation of PMSG. Finally, the simulation model based on MATLAB is built to validate the availability of the proposed control strategy.

Keywords: High voltage direct current grid, Open winding permanent magnet synchronous generator, Wind power generation system, DC/DC converter

1. Introduction

Nowadays, wind energy has become more and more popular due to the energy crisis and environment pollution. And the offshore wind farms have shown more potential due to the better wind energy resource and larger capacity compared with land-based wind farms [1]. To transmit the offshore wind energy to grid with the higher efficiency, the voltage source converter based high voltage direct current (HVDC) system shows the enhanced performance and capability compared with line-commutated converter based HVDC system and high voltage alternating current (HVAC) system [2]-[5].

The variable speed constant frequency wind power generation system is widely used due to the maximum wind energy track capability, in which doubly-fed induction generator (DFIG) and permanent magnet synchronous generator (PMSG) are most widely used [6]-[8]. The wind power generation system based on PMSG is more suitable for offshore wind farms due to the simpler structure, higher generation efficiency and more reliable operation performance [9], [10]. In order to increase the voltage level and capacity of wind power generation system, the open winding PMSG was proposed to achieve the three level voltage control performance with the less current harmonic, which is also helpful to decrease torque ripple to improve the operation reliability. Furthermore, the open winding

PMSG has better fault tolerance capability and can avoid the disadvantage of the neutral voltage rippling compared with traditional PMSG system with three-level VSC scheme [11].

The traditional HVDC system configuration for open winding PMSG based wind power generation system can be shown as Fig. 1 [2], [11], in which the two full scale back to back converters and a step-up transformer are used to transmit the wind energy to the AC grid of wind farm, and a VSC based receiving terminal is used to transmit the overall wind energy to the HVDC system. It can be seen that the four-step power conversion exists from the open winding PMSG to HVDC system, which will lead to complicated structure, low efficiency and high cost.

In order to improve the shortcomings of the traditional HVDC system for open winding PMSG, a novel topology and control strategy of HVDC grid connection for open winding PMSG based wind power generation system is proposed as shown in Fig. 2, in which the grid-side converter and the transformer are eliminated. It can be seen that, two isolated DC/DC converters with series connection are used as power conversion interface between the generator side converter and HVDC system. Therefore, only two-step power conversion is needed to achieve the simpler structure and higher efficiency compared with conventional structure as shown in Fig. 1.

In this paper, the mathematic model of open winding PMSG is deduced based on the rotor flux oriented vector control strategy for open winding PMSG. The space vector pulse width modulation (SVPWM) algorithm for the dual

* Dept. of Electrical Engineering, Zhejiang University, China. (zengh enhli@zju.edu.cn)

** Dept. of Electrical Engineering, Zhejiang University, China. (nianheng@zju.edu.cn)

generator side converters is proposed to achieve a three level voltage vector control scheme. And the isolated DC/DC converter is also controlled by PWM method to keep the DC bus voltage of generator side converter constant. Finally, the availability of the proposed system and control strategy is validated by the simulation based on MATLAB/Simulink.

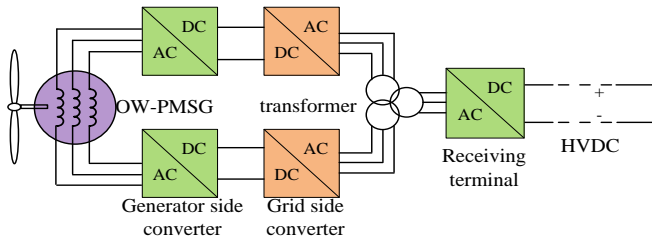


Fig. 1. The traditional HVDC grid connection system for open winding PMSG

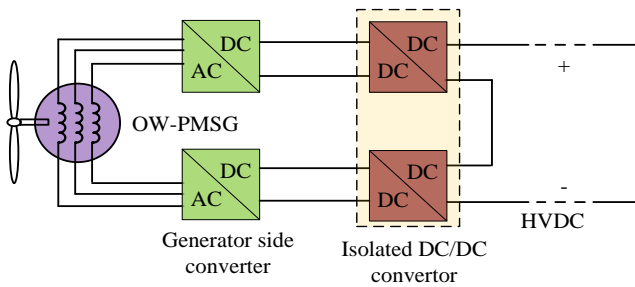


Fig. 2. The novel HVDC grid connection system for open winding PMSG

2. Mathematical Model of open winding PMSG

The proposed configuration shown in Fig. 2 contains an open winding PMSG, two generator side converters and two isolated DC/DC converters. The isolated DC/DC converters are controlled to keep the two DC voltages constant and independent. Thus, the two independent DC voltage sources can be used to develop the open winding PMSG mathematic model, as shown in Fig. 3.

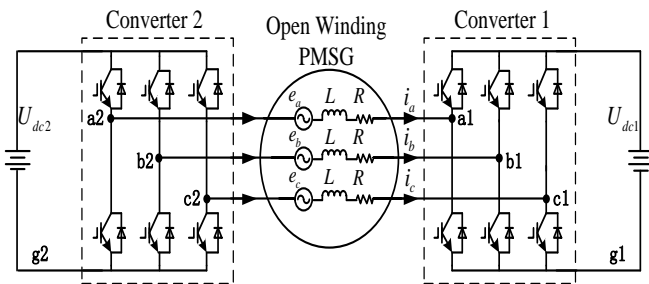


Fig. 3. simplified open winding PMSG system

The phase voltage model of the open winding PMSG can be written as,

$$\begin{cases} u_a = e_a - L \frac{di_a}{dt} - i_a R = S_{a1} U_{dc1} - S_{a2} U_{dc2} + U_{g1g2} \\ u_b = e_b - L \frac{di_b}{dt} - i_b R = S_{b1} U_{dc1} - S_{b2} U_{dc2} + U_{g1g2} \\ u_c = e_c - L \frac{di_c}{dt} - i_c R = S_{c1} U_{dc1} - S_{c2} U_{dc2} + U_{g1g2} \end{cases} \quad (1)$$

where, u is phase voltage, e is back electromotive force (EMF), i is phase current, L is phase inductance, R is phase resistance, S is switching state, in which “1” represents the upper switch is on and “0” represents the lower switch is on, subscript a, b, c represent the three phase components of open winding PMSG, subscript $a1, b1, c1, a2, b2, c2$ separately represent switch condition of three phase bridge arms in the converter 1 and 2, U_{dc1}, U_{dc2} represent DC bus voltage of converter 1 and 2, U_{g1g2} represents voltage between the node $g1$ and $g2$.

As shown in Fig. 3, the two converters are fed by two isolated dc voltage sources respectively. Therefore, the following equation can be deduced as,

$$i_a + i_b + i_c = 0 \quad (2)$$

According to (1) and (2), the phase voltage can be deduced as,

$$\begin{cases} u_a = (S_{a1} - \frac{S_{a1} + S_{b1} + S_{c1}}{3}) U_{dc1} - (S_{a2} - \frac{S_{a2} + S_{b2} + S_{c2}}{3}) U_{dc2} \\ u_b = (S_{b1} - \frac{S_{a1} + S_{b1} + S_{c1}}{3}) U_{dc1} - (S_{b2} - \frac{S_{a2} + S_{b2} + S_{c2}}{3}) U_{dc2} \\ u_c = (S_{c1} - \frac{S_{a1} + S_{b1} + S_{c1}}{3}) U_{dc1} - (S_{c2} - \frac{S_{a2} + S_{b2} + S_{c2}}{3}) U_{dc2} \end{cases} \quad (3)$$

Assuming that the three phase winding of open winding PMSG is symmetry, the phase voltage output by converter 1 can be expressed as,

$$\begin{cases} U_{a1} = (S_{a1} - \frac{S_{a1} + S_{b1} + S_{c1}}{3}) U_{dc1} \\ U_{b1} = (S_{b1} - \frac{S_{a1} + S_{b1} + S_{c1}}{3}) U_{dc1} \\ U_{c1} = (S_{c1} - \frac{S_{a1} + S_{b1} + S_{c1}}{3}) U_{dc1} \end{cases} \quad (4)$$

Then, the phase voltage output by converter 2 can be expressed as,

$$\begin{cases} U_{a2} = (S_{a2} - \frac{S_{a2} + S_{b2} + S_{c2}}{3})U_{dc2} \\ U_{b2} = (S_{b2} - \frac{S_{a2} + S_{b2} + S_{c2}}{3})U_{dc2} \\ U_{c2} = (S_{c2} - \frac{S_{a2} + S_{b2} + S_{c2}}{3})U_{dc2} \end{cases} \quad (5)$$

According to (2), (4) and (5), the phase voltage of open winding PMSG can be rewritten as,

$$\begin{cases} u_a = e_a - L \frac{di_a}{dt} - i_a R = U_{a1} - U_{a2} \\ u_b = e_b - L \frac{di_b}{dt} - i_b R = U_{b1} - U_{b2} \\ u_c = e_c - L \frac{di_c}{dt} - i_c R = U_{c1} - U_{c2} \end{cases} \quad (6)$$

When d-axis is aligned in the rotor flux linkage, the mathematic model of open winding PMSG in the synchronous rotating frame can be represented as,

$$\begin{cases} u_d = u_{d1} - u_{d2} = -i_d R - L_d \frac{di_d}{dt} + \omega_r L_q i_q \\ u_q = u_{q1} - u_{q2} = -i_q R - L_q \frac{di_q}{dt} - \omega_r L_d i_d + \omega_r \Psi_r \end{cases} \quad (7)$$

where, ω_r is the electrical angular speed of open winding PMSG, Ψ_r is the rotor magnetic flux produced by the permanent magnet, subscript d , q represent the d-axis and q-axis component respectively, u_{d1} , u_{q1} and u_{d2} , u_{q2} separately represent the d-axis and q-axis voltage vectors modulated by generator side converter 1 and 2.

Therefore, the active power output P by open winding PMSG and the active power output P_1 and P_2 by converter 1 and 2 can be calculated as the following,

$$\begin{cases} P = \frac{3}{2}(u_q i_q + u_d i_d) = P_1 + P_2 \\ P_1 = \frac{3}{2}(u_{q1} i_q + u_{d1} i_d) \\ P_2 = -\frac{3}{2}(u_{q2} i_q + u_{d2} i_d) \end{cases} \quad (8)$$

And the mathematical model of the mechanical portion

of open winding PMSG can be written as,

$$T_e = \frac{3}{2} n_p (\Psi_r i_d - \Psi_d i_q) \quad (9)$$

$$\frac{J}{n_p} \frac{d\omega_r}{dt} = T_L - T_e \quad (10)$$

where, T_e is the electromagnetic torque, T_L is the driving torque, n_p is the number of pole pairs, J is the inertia of the open winding PMSG.

3. Control Strategy for Proposed System

3.1 Vector Control of Open Winding PMSG

When d axis is aligned in the rotor flux linkage and the vector control of $i_d=0$ control strategy is applied in open winding PMSG, (9) and (10) can be rewritten as,

$$T_e = \frac{3}{2} n_p \Psi_r i_q \quad (11)$$

$$P_e = \omega T_e = \frac{3}{2} \omega n_p \Psi_r i_q \quad (12)$$

It can be seen from (12) that the electromagnetic power is proportional to q-axis current. Thus, it is available to control the output electromagnetic power of the open winding PMSG by regulating q-axis current to implement the maximum power point trace (MPPT).

3.2 SVPWM Modulation Algorithm

The SVPWM method is applied to control the two generator side converters. The voltage space vector modulated by a full-bridge controlled two-level converter can be described as a regular hexagon shown in Fig. 4, which includes six effective vectors and two zero vectors.

Assuming that the two dc sources have the same voltage level, $V_{dc1}=V_{dc2}$ the vector modulated by dual two-level converters can be shown by Fig. 5 according to (13). It can be seen that there are 64 combinations of two converters which are composed of 18 different effective vectors and one zero vector. And V_{12} in Fig. 5 means the combination of converter 1 modulated V_1 and converter 2 modulated V_2 and it is the same with other combinations.

$$\vec{V}_{ref} = \vec{V}_1 - \vec{V}_2 \quad (13)$$

Any vector located in Fig. 5 can be modulated by a proper algorithm which gives the method of coordination of

two converters. For the two dc sources have the same voltage level, $V_{dc1}=V_{dc2}$, let the two converters modulate two equal and opposite vectors to get the maximum utilization of DC voltage, as it is shown in Fig. 6, where the vectors $V_1 V_2$ are equal and opposite.

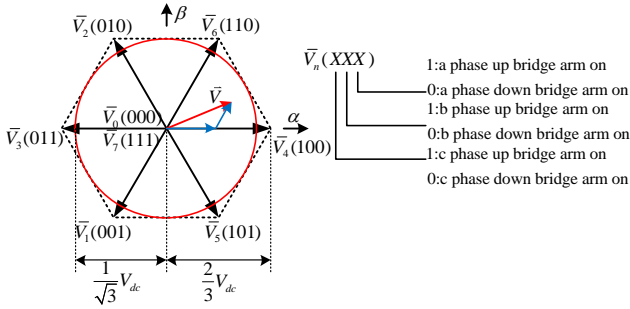


Fig. 4. Space vector locations of two-level converter

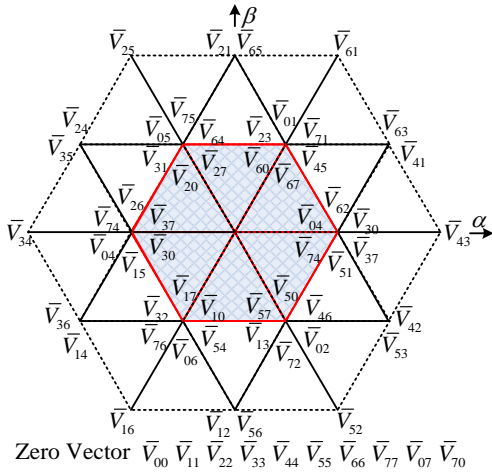


Fig. 5. Space vector locations of dual two-level converters

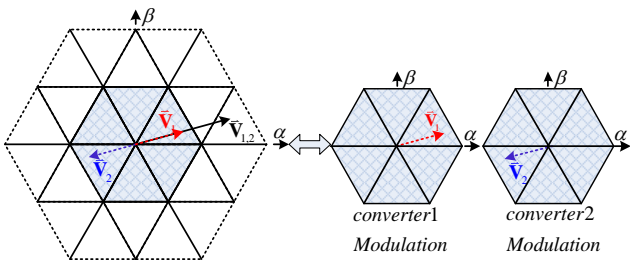


Fig. 6. Proposed algorithm of SVPWM for open winding PMSG

3.3 Control of Isolated DC/DC Converter

In order to implement the wind power transmission from the converter to HVDC grid, two isolated DC/DC converters is applied in the proposed system to isolate open winding PMSG, increase the voltage level and allow series

connection of two terminals. Fig. 7 shows the main circuit of the isolated DC/DC converter which consists of an inductor L , a full-bridge controlled converter constituted of four switches $Q1\sim Q4$, a high frequency transformer with ratio $N (>1)$ and a full-bridge uncontrolled converter constituted of diodes $D1\sim D4$.

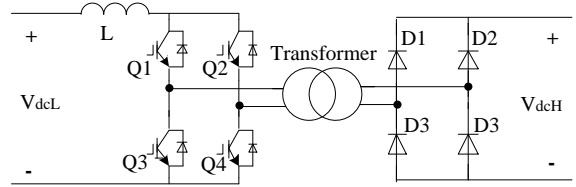


Fig. 7. Configuration of isolated DC/DC converter

To implement the voltage level increase and power transmission from open winding PMSG to HVDC grid, Fig. 8 shows the timing sequence diagram for the DC/DC converter, in which the switch $Q1$ and $Q3$ are controlled by the same PWM, and switch $Q2$ and $Q4$ are controlled by another PWM with 180° phase shift from the PWM of $Q1$ and $Q3$. The duty cycle D can vary from 0 to 1 to regulate the DC bus voltage of the generator side converter by coefficient k_{pwm} . When the duty cycle varies from 0 to 0.5, it works in buck mode $k_{pwm}<1$, and when the duty cycle varies from 0.5 to 1, it works in boost mode $k_{pwm}>1$ ([12]). The ratio of the DC/DC converter can be expressed by coefficient k_{DC} which can be written as,

$$k_{DC} = k_{pwm} \times N \quad (14)$$

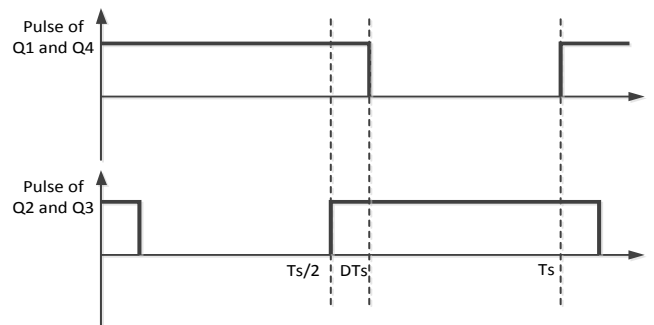


Fig. 8. Timing diagram of Q1~Q4

3.4 Control Diagram of Open Winding PMSG System

The control diagram of the open winding PMSG system is shown in Fig. 9. The vector control of $i_d=0$ control strategy is applied to control the generator side converters, in which the outer loop is power loop and the inner loop is current loop. The q-axis current reference is given by the

output of the power control loop. The reference active power is changed according to the MPPT operation. And the synthetical vector obtained above is distributed to the two generator converters according to (13).

A closed loop control strategy is applied to control the DC/DC converter to maintain the DC bus voltage of the generator side converter (the input voltage of the isolated DC/DC converter) constant. As the output voltage of the isolated DC/DC converter is determined by HVDC system and constant, the input voltage is depended on the coefficient k_{pwm} as the ratio of the transformer N is fixed. Thus, a voltage loop with proportional-integral (PI) regulator is designed for the DC/DC converter to maintain the input voltage constant by adjusting the duty cycle as shown in Fig. 9.

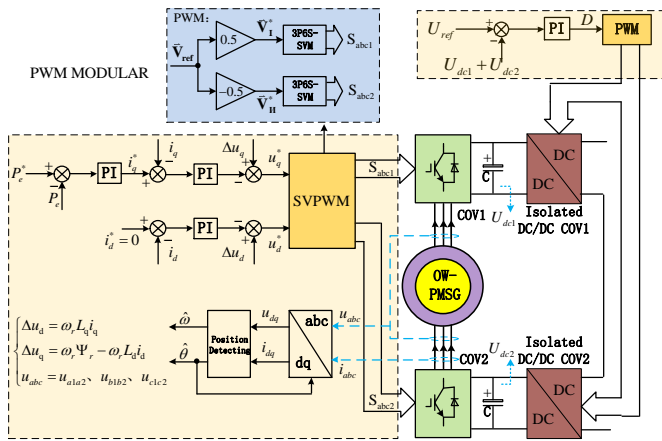


Fig. 9. Control diagram of open winding PMSG system

4. Simulation

To validate the proposed system scheme and control strategy for open winding PMSG system, the simulation study based on MATLAB with a 2MW system is built. The electrical and mechanical parameters are shown in Table 1.

Table 1. PARAMETERS FOR OPEN WINDING PMSG SYSTEM

Data	Code	Value
Rated Power	P_n	2MW
Rated Voltage	U_n	690V
Rated Current	I_n	1604.6A
Rated Frequency	f_n	14.4Hz
Rated Speed	ω_n	18r/min
Stator Resistance	R	$3.52e-3\Omega$
d-axis inductance	L_d	$2.54e-4H$
q-axis inductance	L_q	$2.54e-4H$
Poles pairs	n_p	48
Low DC Voltage	V_{dcL}	600V

High DC Voltage	V_{dcH}	5kV
Switching Frequency	f_{PWM}	2KHz

When the system works at rated operation state, the input of the wind speed is 11m/s, and the line voltages modulated by converter1, 2 and the phase voltage of the open winding PMSG in steady operation state is shown in Fig. 10. It can be seen that the dual inverter modulation has three-level modulation effect. The FFT analysis result of a phase voltage U_{a1a2} is shown in Fig. 11 and it can be noted that the THD is 9.39% and mainly contributed by high frequency harmonic on the multiples of switching frequency.

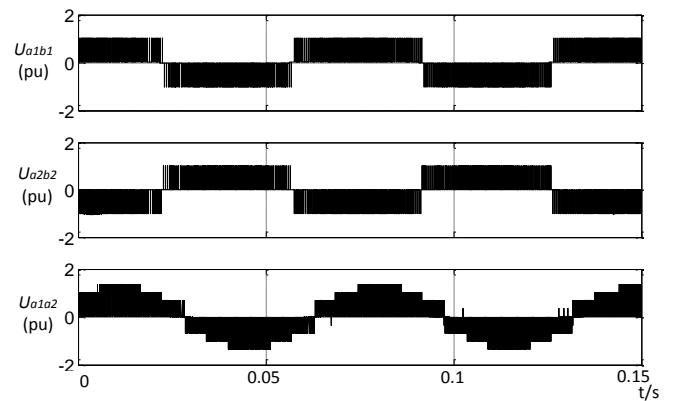


Fig. 10. Voltage waveforms at rated operation state (a) a/b phase-phase voltage modulated by inverter1 (b) a/b phase-phase voltage modulated by inverter2 (c) a phase voltage of the open winding PMSG

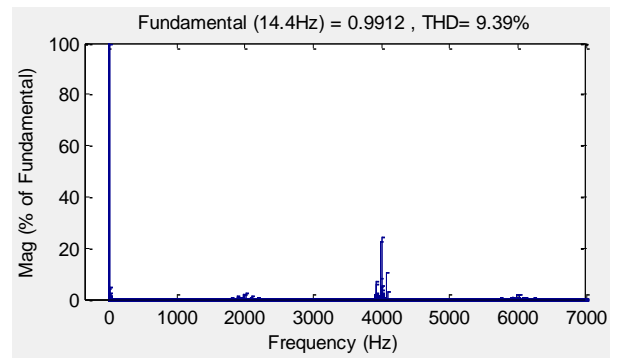


Fig. 11. FFT analysis result of a-phase voltage U_{a1a2}

Fig.12 shows simulation results of the proposed system at the rated operation state. The output dc voltages of generator side converters are both steady at 600V in Fig. 12 (a) and (b), which verifies the effectiveness of the control strategy of the isolated DC/DC converters. And it can be noted from Fig.12 (c), (d), (e), and (g) that the active and reactive power of converter 1, converter 2 and open winding PMSG and the torque of open winding PMSG is

steady. In Fig. 12, $P1$, $Q1$ and $P2$, $Q2$ represent the active and reactive power output by converter 1 and converter 2 respectively, and P , Q represent the active and reactive power output by open winding with $\pm 0.04pu$ and $\pm 0.03pu$ fluctuation respectively. In addition, the phase currents is shown in Fig. 12 (f), and the FFT analysis of a-phase current obtains that THD is only 0.66% which prove the excellent performance of the proposed system. The steady state with power and torque validates the availability and effectiveness of the proposed system and control strategy at the rated operation condition.

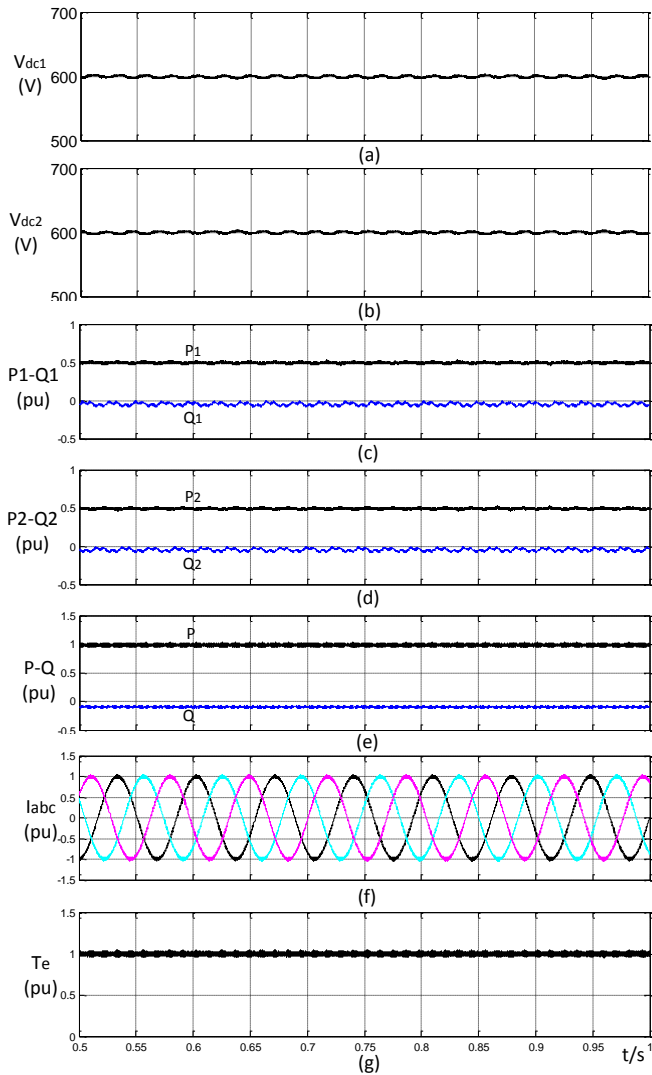


Fig. 12. the results of simulation at the rated operation state
 (a) The output DC voltage of converter1
 (b) the output voltage of converter2
 (c) Active and reactive power output by converter1
 (d) active and reactive power by converter2
 (e) active and reactive power output by motor
 (f) Three-phase current of the open winding PMSG
 (g) The electromagnetic torque of the open winding PMSG

Fig. 13 shows the dynamic performance of the proposed open winding PMSG system, in which the wind speed changes from 11m/s to 9m/s at the period of 1.0s to 1.1s

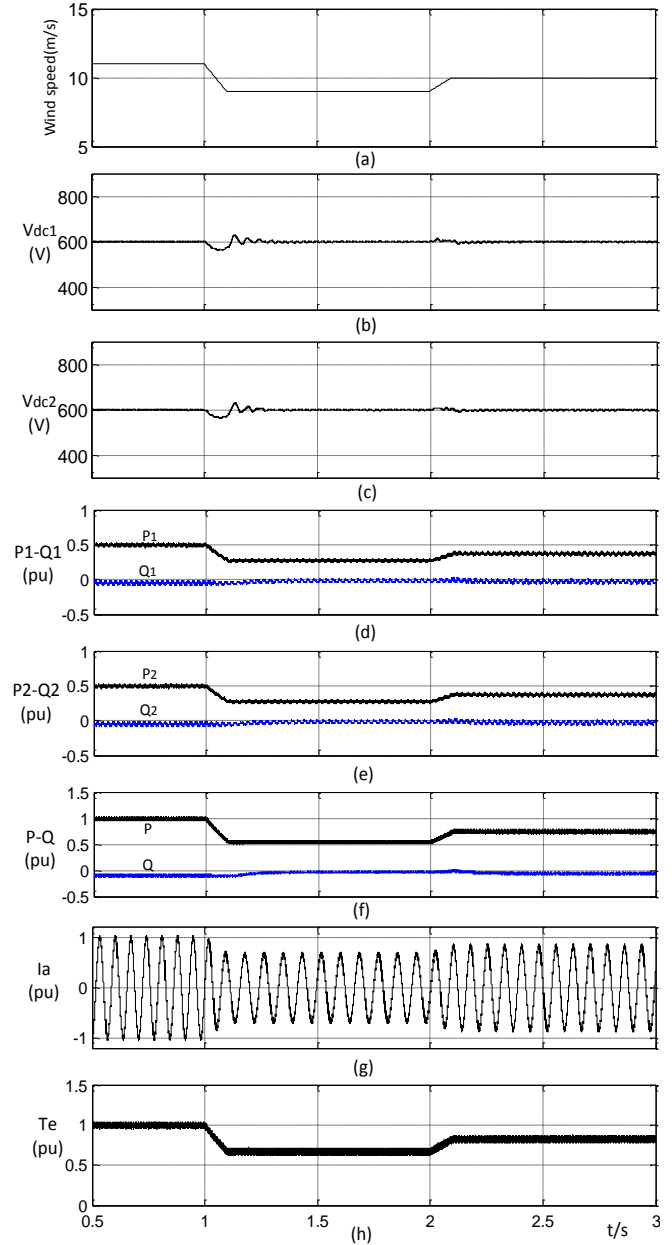


Fig. 13. the results of simulation with dynamic wind speed
 (a) The reference of wind speed
 (b) DC voltage output by converter1
 (c) DC voltage output by converter2
 (d) Active and reactive power output by converter1
 (e) Active and reactive power by converter2
 (f) Active and reactive power output by motor
 (g) The a-phase current of the open winding PMSG
 (h) The electromagnetic torque of the open winding PMSG

and from 9m/s to 10m/s at the period of 2.0s to 2.1s. It can be seen that the output voltages of the generator side converters, active and reactive power, and torque can reach a steady state within 0.3s after wind speed changed, which validate the availability and effectiveness of the proposed system and control strategy with dynamic wind speed. And the power is steady at 0.55pu and 0.75pu respectively when wind speed changed to 9m/s and 10m/s. The system can achieve the MPPT with the wind speed and power having cube relationship. Thus, the steady performance of the simulation illustrates the availability and effectiveness of the proposed system and control strategy with dynamic wind speed reference.

5. Conclusion

A novel topology and control strategy of HVDC grid connection for open-winding PMSG based wind power generation system is proposed in this paper. There is two-step power conversion from generator to HVDC with generator-side converters and isolated DC/DC converters, which leads to the simpler structure and higher efficiency than the traditional system which has four-step power conversion. And the rotor flux oriented vector control strategy based on SVPWM method is designed for the motor by deduced the mathematic model of open winding PMSG. The simulation of the system based on MATLAB is built and the results at rated operation state and dynamic reference of wind speed state validate the availability and effectiveness of the proposed system and control strategy.

References

[1] B. Snyder, M. J. Kaiser, "Ecological and economic cost-benefit analysis of offshore wind energy," *Renewable Energy*, vol.34, no.6, 2009, pp.1567-1578.

[2] Kun Zhao, Gengyin Li, Bozhong Wang and Ming Zhou, "Grid-Connected Topology of PMSG Wind Power System Based on VSC-HVDC," in *Proc. 2011 4th International Conference on Electric Utility Deregulation and Restructuring and Power Technologies*, 2011, pp. 297-302.

[3] Xiaodong Zhu, Keliang Zhou, Ming Cheng, Xiaofan Fu, Wei Wang, Tong Wang, "Topologies and control of VSC-HVDC systems for grid-connection of large-scale offshore wind farms," *Power System Technology*, vol. 33, no. 18, 2009, pp. 17-24.

[4] Gengyin Li, Pengfei Lv, Guankai Li, Ming Zhou, "Development and prospects for HVDC light," *Automation of Electric Power Systems*, vol. 27, no. 4, February 2003, pp. 77-81.

[5] N. Negra, J. Todorovic, T. Ackermann, "Loss evaluation of hvac and hvdc transmission solution for

large offshore wind farms", *ELSEVIER Electric Power System Research*, no.76, 2005, pp.916-927.

[6] M. Chinchilla, S. Arnaltes, J. Burgos, "Control of permanent-magnet generators applied to variable-speed wind-energy systems connected to the grid," *IEEE Transaction on Energy Conversion*, vol.21, no.1, 2006, pp. 130-135.

[7] S. M. Muyeen, R. Takahashi, T. Murata, J. Tamura, "A Variable Speed Wind Turbine Control Strategy to Meet Wind Farm Grid Code Requirement," *IEEE Transaction on Power System*, vol.25, Issue 1, 2010, pp. 331-340.

[8] Fengxiang Wang, Yue Zhang, Yongshan Shen, "Comparison of different structures for variable speed constant frequency wind power generator," *Electrical Machines and Systems (ICEMS), 2008 International Conference on*, 2008, pp. 2234-2238.

[9] Ke Xu, Chao Wu, Xiaojing Yang, Minqiang Hu, "Structure analysis and control of wind power generation in VSC-HVDC," *Power System Technology*, vol. 33, no. 4, 2009, pp. 103-108.

[10] H. Polinder, F. F. A van der Pijl, G. J. de Vilder, "Comparison of direct-drive and geared generator concepts for wind turbines," *IEEE Trans. Energy Convers*, vol.21, no.3, 2006, pp.725-733.

[11] Yijie Chou, Heng Nian, "Sensorless control of PMSG based on dual two-level inverter open winding configuration for wind turbines," *Electrical Machines and Systems (ICEMS), 2012 International Conference on*, On Page(s): 1-6.

[12] Xuesong Jiang, Xuhui Wen, Haiping Xu, "Study on Isolated Boost Full Bridge Converter in FCEV," *Power Engineering Conference, 2005, The 7th International IPEC 2005*, 2005, pp.827-830.



Hengli Zeng received B.S degree in electrical engineering in 2012 and is pursuing his master degree in Zhejiang University. His research interests are the DC grid connection technology for open winding PMSG based wind power generation system.



Heng Nian received the B.Eng. degree and the M.Eng. degree from HeFei University of Technology, China, and the Ph.D. degree from Zhejiang University, China, in 1999, 2002, and 2005 respectively, all in electrical engineering.

From 2005 to 2007, he was as a Post-Doctoral with the College of Electrical Engineering, Zhejiang University, China. Since 2007, he has been employed as an associate professor at the College of Electrical Engineering, Zhejiang University, China. Current research interests are the optimal design and operation control for wind power generation system.